

Spatial variability of *Mycosphaerella coffeicola* (Cooke) populations in coffee plantations, State of Mexico

Dulce Karen Figueroa-Figueroa¹

Fidel Lara-Vázquez²

José Francisco Ramírez-Dávila^{2,§}

Aurelio Pérez-Constantino²

Agustín David Acosta-Guadarrama¹

Federico Benjamín Galacho-Jiménez³

1 Unidad de Estudios Superiores Coatepec Harinas-Universidad Mexiquense del Bicentenario.

Ejido San Luis, El Reynoso, Coatepec Harinas, Estado de México. CP. 51700. Tel. 722 5185660.

(dulce.figueroa@umb.mx; agustin.acosta@umb.mx).

2 Facultad de Ciencias Agrícolas-Universidad Autónoma del Estado de México. Carretera Toluca-Ixtlahuaca km 15.5, El Cerrillo Piedras Blancas, Toluca. Estado de México. CP. 50295. Tel. 722 2965529. (flarav-s@uaemex.mx; pajes-aure@hotmail.com).

3 Departamento de Geografía-Universidad de Málaga. Grupo de Análisis Geográfico, Málaga, España. CP. 29071. Tel. 952 132172. (fbgalacho@uma.es).

Autor para correspondencia: jframirez@uaemex.mx.

Abstract

Coffee is an important crop in Mexico and the State of Mexico is a producing state affected by the iron spot disease caused by the fungus *Mycosphaerella coffeicola*; this disease reduces the synthetic area, causes defoliation and can affect the quality of beans. Its control is limited due to the lack of knowledge of its spatial distribution within the plots. This study determined the distribution of iron spot in coffee using geostatistical techniques. Semivariograms and distribution maps were made by ordinary kriging, estimating the infested area. The incidence varied and correlated with temperature and relative humidity. An aggregate distribution that fitted theoretical models (Gaussian and spherical) was observed. Infestation was not uniform in the plots, suggesting that targeted control can optimize costs and improve the sustainability of crop management.

Keywords:

Mycosphaerella coffeicola, aggregation, geostatistics, ordinary kriging, semivariograms.



Introduction

Mexico has more than 500 000 coffee producers in 700 000 ha, being the ninth largest producer in the world (SIAP, 2023). The State of Mexico has gained recognition for the quality of its grain (Cup of excellence, 2022a; 2022b; 2022c). Iron spot is a major disease in coffee, causing defoliation and reducing bean quality (Rengifo *et al.*, 2002). Kermack and McKendric (1927) contributed to understanding the dynamics of diseases with mathematical knowledge applied to different scientific fields, one of which is agriculture, where this makes it possible to understand and predict the spatial behavior of pests and diseases (Tapia, 2020). Pérez (2023) mentions that, in order to carry out efficient and adequate phytosanitary management, it is necessary to know the spatial and temporal behavior of pests or diseases, so the use and knowledge of spatial modeling tools and techniques become necessary. Spatial geostatistics has been used in the spatial analysis of plant health and its interaction with the environment and other abiotic variables (Tapia, 2020). In this context, geostatistical methods have been applied to evaluate its distribution, with the aim of determining the spatial variability of *Mycosphaerella coffeicola* in Temascaltepec, State of Mexico.

Materials and methods

Study area

The study was conducted in Temascaltepec ($19^{\circ} 02' 3''$ north latitude, $100^{\circ} 02' 29''$ west longitude, 1 719 masl); four plots with Caturra and Typica varieties were selected. Biweekly sampling was carried out from 2021 to February 2022.

Each plot (0.5 ha) was divided into 50 quadrants, selecting 200 shrubs at random, georeferenced with GPSmap60 (Garmin). In each shrub stratum (high, low, medium), damaged leaves were counted on primary branches oriented to the four cardinal points (Ramírez-Dávila *et al.*, 2011; Acosta-Guadarrama *et al.*, 2017; Lara *et al.*, 2018).

To identify the fungus, samples were isolated in specific culture media (Tapia-Rodríguez *et al.*, 2020) and morphological characterization of monoconidial strains was performed, which were reseeded in (CAA) and placed in an incubator at 24°C . Taxonomic keys were used (Chand *et al.*, 1954).

Climatic elements

Temperature and relative humidity were recorded with a Hobo Pro V2 Datta Loger placed in each plot.

Geostatistical analysis

Experimental semivariograms fitted to spherical, exponential, Gaussian, linear and penta-parametric models were generated with Variowin 2.2 (Software for spatial data analysis) (Ramírez, 2011). Spatial dependence was evaluated and values were interpolated using ordinary kriging, estimating values associated with points not sampled and represented on maps in Surfer 16 (Surface Mapping System, Golden Software Inc., Golden) (Cambardella *et al.*, 1994). The maps were used to estimate the infested area to consider an economic and environmental assessment of directed agriculture (Ramírez-Dávila *et al.*, 2008; Tapia-Rodríguez *et al.*, 2020).

Results and discussion

Pathogen identification

Morphological analysis confirmed the presence of *Mycosphaerella coffeicola*. Observations in light microscopy revealed hyaline to slightly pigmented, multicellular, thread-shaped conidia with sharp

ends and typical transverse septations measuring 30-200 µm long and 2.5-5 µm wide, values that are similar to those reported for *Cercospora coffeicola* (Chand *et al.*, 1954).

Climatic elements

The temperature ranged from 18 °C in January to 25.9 °C in September, with relative humidity of 44% to 90%. The epidemiological triangle is a concept that is applied to diseases and pests in crops. The three key components for propagation and persistence, according to Pérez (2023), three factors must coexist: host (coffee), causal agent (iron spot) and favorable conditions that encompass all abiotic factors (soil, management, variety, climate, among others).

Likewise, Guzmán *et al.* (2008) indicate that iron spot affects the plant in all stages of development and causes loss of fruit weight, deterioration of quality and a high percentage of deficient production; on the other hand, Guzmán-Piedrahita and Rivillas-Osorio (2005) mention that the temperature ranges between 18 and 28 °C, with an optimum of 25 °C, and 70 and 100% in relative humidity with an optimum of 98%; for her part, Arteaga-Luna (2013) points out that the disease is more favored by high humidity, high temperature, and water stress, when temperatures vary between 18 and 25 °C, incubation lasts 24 to 25 days.

The temperature for conidia germination is 30 to 34 °C. Guzmán-Piedrahita and Rivillas-Osorio (2005) indicate the importance of some climatic factors, such as precipitation, temperature, and relative humidity.

Geostatistics

The semivariograms fitted the following models: Gaussian 37.5% (18 of 48), spherical 43.75% (21 of 48), and exponential 18.7% (9 of 48) (Table 1). The geostatistical parameters allowed the validation of semivariograms. All the semivariograms of the models obtained were determined to have a nugget effect equal to zero (Table 1).

Table 1. Parameters of the theoretical models fitted to the semivariograms of *Mycosphaerella coffeicola*, in the municipality of Temascaltepec.

Pl. 1	Me	Va	Mo	Nu	Si	Ra	N/S	SD	Pl. 2	Me	Va	Mo	Nu	Si	Ra	N/S	SD
1. S1	6.01	42.86	Spherical	0	72.8	10.8	0	High	1. S1	5.67	40.33	Gaussian	0	29.7	4.6	0	High
2. S2	5.84	40.06	Exponential	0	67.16	10.2	0	High	2. S2	5.62	38.48	Exponential	0	21.32	3.64	0	High
3. O1	5.79	37.97	Spherical	0	64.6	6.75	0	High	3. O1	5.49	39.68	Gaussian	0	20.91	3.77	0	High
4. O2	5.75	36.22	Exponential	0	62.4	8.32	0	High	4. O2	5.46	36.14	Gaussian	0	19.6	3.51	0	High
5. N1	5.69	35.36	Spherical	0	60.48	6.76	0	High	5. N1	5.39	35.78	Gaussian	0	18.24	3.38	0	High
6. N2	5.64	34.21	Spherical	0	58.56	7.84	0	High	6. N2	5.38	34.75	Exponential	0	17.86	3.38	0	High
7. D1	5.6	33.59	Exponential	0	58.2	9.52	0	High	7. D1	4.97	30.28	Gaussian	0	17.63	4.59	0	High
8. D2	5.52	32.32	Spherical	0	55.29	8.5	0	High	8. D2	4.89	29.16	Gaussian	0	14.82	3.51	0	High
9. E1	5.46	31.39	Spherical	0	54.45	7.19	0	High	9. E1	4.76	26.28	Gaussian	0	13.65	3.25	0	High
10. E2	5.46	31.4	Spherical	0	54.45	7.84	0	High	10. E2	4.74	24.94	Exponential	0	11.52	3.25	0	High
11. F1	5.37	29.66	Spherical	0	48.96	7.2	0	High	11. F1	4.52	24.78	Gaussian	0	10.56	2.99	0	High
12. F2	5.2	26.95	Spherical	0	45.08	8.8	0	High	12. F2	4.22	21.65	Gaussian	0	10.5	2.99	0	High
Pl. 3	Me	Va	Mo	Nu	Si	Ra	N/S	SD	Pl. 4	Me	Va	Mo	Nu	Si	Ra	N/S	SD
1. S1	4.64	24.47	Spherical	0	39.56	7.56	0	High	1. S1	4.03	12.72	Spherical	0	17.82	6	0	High
2. S2	4.47	23.14	Spherical	0	35.28	4.25	0	High	2. S2	3.58	11.66	Spherical	0	16.8	5.4	0	High
3. O1	4.5	20.58	Exponential	0	30.26	5	0	High	3. O1	3.11	10.41	Gaussian	0	16	4	0	High
4. O2	4.25	20.34	Spherical	0	27.84	5	0	High	4. O2	3.02	9.82	Gaussian	0	15.39	4	0	High
5. N1	4.18	20.2	Exponential	0	26.1	5.5	0	High	5. N1	2.93	9.62	Gaussian	0	15.12	4	0	High
6. N2	4.13	20.01	Spherical	0	24.64	5.25	0	High	6. N2	2.88	9.31	Gaussian	0	14.76	4.4	0	High
7. D1	3.98	19.97	Exponential	0	24.64	5.25	0	High	7. D1	2.74	8.97	Gaussian	0	14.28	4.4	0	High

Pl. 1	Me	Va	Mo	Nu	Si	Ra	N/S	SD	Pl. 2	Me	Va	Mo	Nu	Si	Ra	N/S	SD
8. D2	3.88	19.71	Spherical	0	23.46	5.5	0	High	8. D2	2.41	8.17	Gaussian	0	13.6	4.4	0	High
9. E1	3.81	18.54	Spherical	0	23.49	5.5	0	High	9. E1	2.36	7.91	Gaussian	0	12.6	4.4	0	High
10. E2	3.72	17.75	Spherical	0	22.62	5.25	0	High	10. E2	2.18	7.67	Spherical	0	10.95	5.46	0	High
11. F1	3.7	17.25	Spherical	0	22.36	5.25	0	High	11. F1	1.98	6.95	Gaussian	0	10.27	4.4	0	High
12. F2	3.25	17.17	Spherical	0	21.25	5	0	High	12. F2	1.8	6.14	Gaussian	0	10.08	4.4	0	High

Pl= plot; Me= mean; Va= variance; Mo= model; Nu= nugget; Si= sill; Ra= range; N/S= nugget/sill; SD= spatial dependence.

The high level of spatial dependence resulted from dividing the value of the nugget effect by the value of the sill, which was less than 25% for all semivariograms. The values of the range or scope ranged from 6.75 to 10.8 m for plot one, and regarding plot two, they ranged from 2.99 to 4.6 m (Table 1). These ranges are the maximum distance up to which there is a relationship between the data.

The maps made based on the ordinary kriging method are shown in Figures 1 and 3. In the maps made, it is possible to distinguish the different points of aggregation of incidence of iron spot disease in the four plots studied; it should be noted that, with these maps, we can visually identify how the disease behaves spatially with respect to time and soil and climatic requirements.

Figure 2. Map of infection density of iron spot *Mycosphaerella coffeicola*, plots one and two of the municipality of Temascaltepec, State of Mexico.

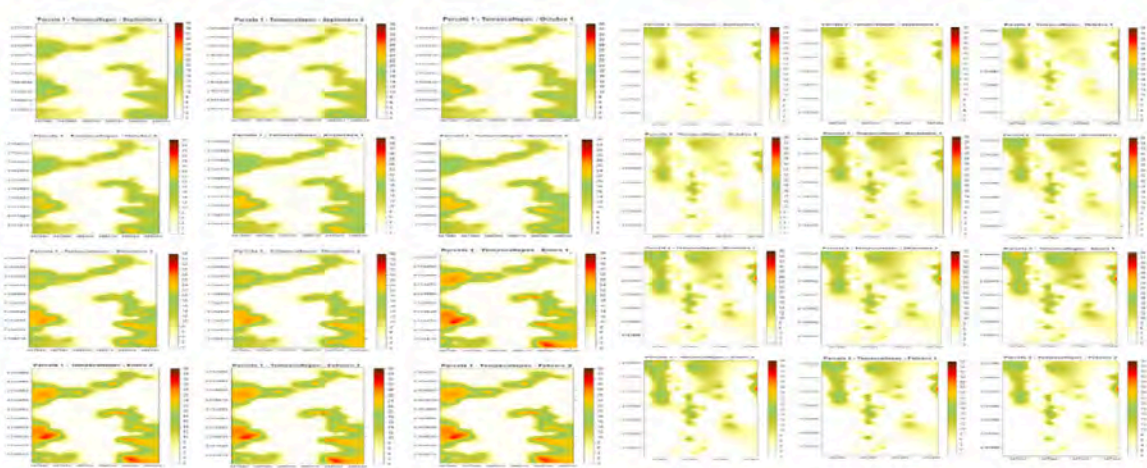
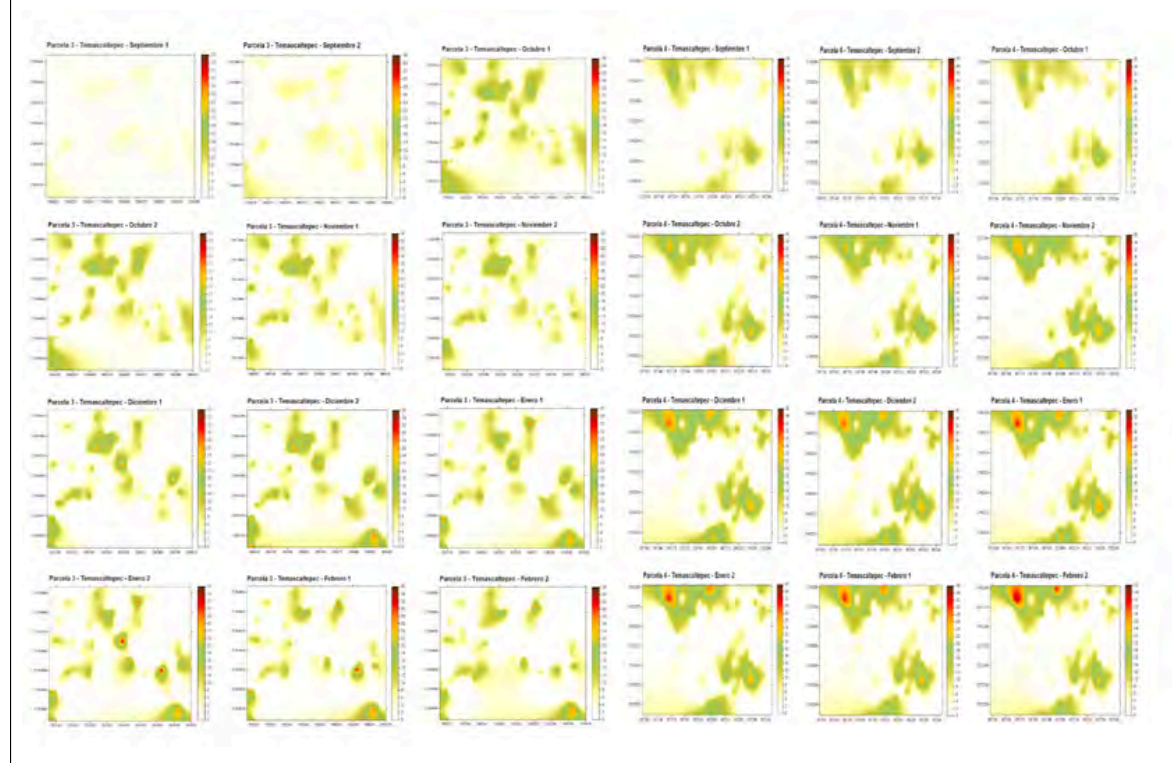


Figure 3. Map of infection density of iron spot *Mycosphaerella coffeicola*, plots three and four of the municipality of Temascaltepec, State of Mexico.



The spatial variability of the iron spot was determined through the use of geostatistics; the results agree with other authors, such as Ramírez *et al.* (2011), who indicate that the geostatistical analysis was appropriate for modeling and mapping the spatial distribution of corn head smut; on the other hand, Turechek and Madden (1999) point out that, through geostatistics, they carried out the spatial modeling of the damage caused by the disease *Mycosphaerella fragariae* in strawberry leaves on different dates; likewise, Sciarretta *et al.* (2008) indicate that, through geostatistics, they identified the spatial distribution of *Lobesia botrana* in grape plots.

Regarding the semivariograms that fitted the Gaussian models, these indicate that the behavior of iron spot disease in the plots was continuous, since the infestation of the fungus, in terms of its advance, is among the neighboring trees, which suggest that it begins leaf by leaf; this phenomenon was observed by Tapia-Rodríguez *et al.* (2020) in anthracnose in avocado crops, which presents an aggregate spatial distribution in the crop, with semivariograms that fitted the Gaussian model, interpreting that the disease presents an accelerated growth over time continuously.

In the study by Acosta-Guadarrama *et al.* (2017) in thrips, the adjustment was mainly Gaussian, which indicates a continuous expression of the insect within avocado plantations.

On the other hand, the models fitted to the spherical model indicate that iron spot populations are mostly present in certain areas of the plot compared to the rest of the points considered in the sampling, that is, the aggregation centers are random within the infestation zone in the plot; Esquivel and Jasso (2014) pointed out that, in the semivariograms fitted to the spherical model, armyworm aggregation centers are random within the infestation zone, with rapid growth close to the source.

Finally, the exponential models indicate that aggregation in the disease occurs in irregular boundaries in the plot, showing a discontinuous spatial distribution; likewise, Ramírez-Dávila *et al.* (2011) point out that the exponential models that were obtained in the *B. cockerelli* samplings presented specific points within the plot in a discontinuous manner; on the other hand, Paz and Arrieché (2017) indicate that, with the samplings carried out on *Thrips tabaci*, they obtained

exponential models, concluding that the special distribution responds to an aggregate pattern, going from dispersed areas to well-defined areas.

Regarding the nugget effect, in all models, it was equal to zero, allowing us to consider that the error was minimal and the sampling scale was appropriate (Ramírez-Dávila *et al.*, 2011; Tapia-Rodríguez *et al.*, 2020). The high level of spatial dependence is known through the value resulting from dividing the value of the nugget effect by the value of the sill, indicating less than 25% in all samplings.

The values show a high spatial dependence, which indicates that the patches of iron spot infection depend on each other and their level of aggregation. This was also observed by Maldonado *et al.* (2016), who point out that the spatial distribution of thrips is similar to that of iron spot.

Infected area

Table 2 details the results obtained in the municipality of Temascaltepec with respect to the infested area; it can be seen that in no sampling did the infection reach 100%; regarding the highest percentage, this was registered at 70%, which was the case of plot three in sampling six; the lowest percentages were registered at 53%, in plot four sampling eleven; the above is relevant for the integrated management of iron spot in the coffee plantations of the municipality of Temascaltepec since it will allow direct applications on specific areas of infection.

Table 2. Percentage of area infested and not infested by iron spot.

Date	Plot 1		Plot 2		Plot 3		Plot 4	
	In ar (%)	Unin ar (%)						
1) Sep 1	60	40	64	36	67	33	56	44
2) Sep 2	61	39	66	34	68	32	58	42
3) Oct 1	62	38	66	34	69	31	59	41
4) Oct 2	62	38	67	33	69	31	59	41
5) Nov 1	62	38	67	33	69	31	59	41
6) Nov 2	63	37	67	33	70	30	60	40
7) Dec 1	61	39	65	35	69	31	58	42
8) Dec 2	60	40	64	36	67	33	57	43
9) Jan 1	60	40	63	37	67	33	57	43
10) Jan 2	59	41	63	37	66	34	56	44
11) Feb 1	58	42	62	38	65	35	53	46
12) Feb 2	58	42	61	39	65	35	54	46

In ar= infested area; Unin ar= uninfested area.

Once the corresponding theoretical semivariograms were validated, the geostatistical method called ordinary kriging was used to make the density maps, allowing us to visualize the behavior of the aggregation foci in the sampled plots; in this sense, in their work on spatial distribution of *Mycena citricolor* in coffee plantations, Pino-Miranda *et al.* (2022) generated maps through the ordinary kriging, estimating the percentages of infected area and the values associated with unsampled points; on the other hand, according to Cárdenas *et al.* (2017), in their spatial study on the incidence of diseases in different types of cocoa, kriging maps allow us to estimate the spatial distribution of areas of influence with specific levels of prevalence. Other authors, such as Lara *et al.* (2018), indicate that the maps obtained with the ordinary kriging technique allow us to identify the places where the populations are concentrated since an interpolation describing the spatial variation is made and there is a predictive capacity.

This generated both ecological and economic benefits as the frequency of pesticide application is reduced, fuel is saved, and more precise management can be done with these maps. Table 2 shows the percentage of the area infested by iron spot, and it can be observed that the distribution of the aggregation of the incidences or foci of iron spot infestation at no time infested the entire plot.

A study by García and Flego (2008) indicates that precision agriculture is based on applying the right amount of inputs at the right time and in the right place, involving the use of global positioning systems (GPS) and other electronic means to obtain crop data.

The maps generated through kriging allow us to identify foci of infection of diseases and thus contribute to accurate and timely decision-making, contributing to the generation of integrated management strategies; according to Sepúlveda (2016), the control of the fungus *Mycosphaerella* requires the application of an increasing number of fungicides due to the resistance that this pathogen has developed; on the other hand, Pérez (2023) points out that, with the use of infestation maps, producers can be suggested to carry out an integrated management of the pest, in which control methods, such as biological and cultural, different from chemical, can be used, greatly reducing contamination to the environment.

Conclusions

The presence of *Mycosphaerella coffeicola* was detected in all the months sampled; nevertheless, its incidence was variable between months, which was related to changes in temperatures, rainfall, and relative humidity. The iron spot presented an aggregate spatial behavior, being found in clearly determined aggregation centers, which remained constant during the six months of sampling; the spatial distribution fitted Gaussian, exponential and spherical models, allowing us to explain spatial dependence.

With the ordinary kriging technique, the aggregation centers can be visualized, making it possible to know their behavior in real time; it allows us to visualize the population variability, being able to conduct the management accurately with these maps.

Bibliography

- 1 Acosta-Guadarrama, A. D.; Ramírez-Dávila J. F.; Rivera-Martínez R.; Figueroa-Figueroa, D. K.; Lara-Díaz, A. V.; Maldonado-Zamora, F. I.; Tapia-Rodríguez, A. 2017. Distribución espacial de *Trips* spp. (Thysanoptera) y evaluación de su control mediante el depredador *Amblyseius swirskii* en el cultivo de aguacate en México. Entomólogo del Suroeste. 42(2):435-446. <https://doi.org/10.3958/059.042.0214>.
- 2 Arteaga-Luna, S. P. 2013. Eficacia de dos productos a base de Trichoderma, en tres dosis de aplicación para el control de la mancha de hierro (*Cercospora coffeicola*) en plantas de café (*Coffea canephora*) Variedad robusta a nivel de vivero en el cantón. Francisco de Orellana, provincia de Orellana Bachelor's . tesis de pregrado, maestría o doctoral, Escuela Superior Politécnica de Chimborazo. <http://dspace.espoch.edu.ec/handle/123456789/4828>.
- 3 Chand, R.; Singh, V.; Kumar, P.; Pal, C. and Chowdappa, P. 1954. The genus Cercospora: biology and taxonomy. Fungal leaf spot diseases of annual and perennial crops. Westville Publishing House, New Delhi. 2-8 pp.
- 4 Cambardella, C.; Moorman, T.; Novak, J.; Parkin, T.; Karlen, D.; Turco, R. and Konopka A. 1994. Field scale variability of soil properties in central Iowa soils. Soil Sci. Soc. Am. J. 58(5):1501-1511. Doi:10.2136/sssaj1994.03615995005800050033x.
- 5 Cárdenas, N. J.; Darghan, A.; Sosa, M. D. y Rodríguez, A. 2017. Análisis espacial de la incidencia de enfermedades en diferentes genotipos de cacao (*Theobroma cacao L.*) en El Yopal (Casanare), Colombia. Acta Biológica Colombiana. 22(2):209-220. Doi: <http://dx.doi.org/10.15446/abc.v22n2.61161>.
- 6 Cup of Excellence. 2022a. Ganadores Nacionales. 2022. <https://cupofexcellence.org/mexico-2021/>.
- 7 Cup of Excellence. 2022b. Ganadores Nacionales. 2022. <https://cupofexcellence.org/mexico-2019/>.
- 8 Cup of Excellence. 2022c. Ganadores Nacionales. 2022. <https://cupofexcellence.org/mexico-2018>.

- 9 Esquivel, H. V. y Jasso, G. Y. 2014. Distribución espacial y mapeo de gusano soldado en seis localidades del Estado de México, en el año 2011. Revista Mexicana de Ciencias Agrícolas. 5(6):923-935. <https://doi.org/10.29312/remexca.v5i6.879>.
- 10 García, E. y Flego, F. 2008. Agricultura de precisión. Revista Ciencia y Tecnología. 8:99-116. <https://www.foroconsultivo.org.mx/incytu/documentos/expres/ie015agricultura%20de%20precision.pdf>.
- 11 Guzmán, O. A. y Rivillas, L. A. 2008. Relación de *Glomus manihotis* y *G. fasciculatum* con el crecimiento de plantas de café y la severidad de la mancha de hierro. Revista del Centro Nacional de Investigaciones de Café Cenicafé. 58(3):236-251. [https://www.cenicafe.org/es/publications/arc058\(03\)236-257.pdf](https://www.cenicafe.org/es/publications/arc058(03)236-257.pdf).
- 12 Guzmán-Piedrahita, O. A. y Rivillas-Osorio, C. A. 2005. Producción *in vitro* de conidios de *Cercospora coffeicola*. Cenicafé. 56(1):67-78. [https://www.cenicafe.org/es/publications/arc056\(01\)067-078.pdf](https://www.cenicafe.org/es/publications/arc056(01)067-078.pdf).
- 13 Kermack, W. O. and McKendrick, A. G. 1927. Contributions to the mathematical theory of epidemics. Proceedings of the Royal Society of London. 115:700-721. <https://www.jstor.org/stable/94815>.
- 14 Lara, F.; Ramírez, J. F.; Rubí, M.; Morales, E. J.; Figueroa, D. K.; Acosta, A. D. y Rivera, R. 2018. Distribución espacial de araña roja *Oligonychus punicae* Hirst en el cultivo del aguacate, en dos municipios del Estado de México. Southwestern Entomologist. 43(3):743-759. Doi: <https://doi.org/10.47163/agrociencia>.
- 15 Maldonado, F. I.; Ramírez, J. F.; Rubí, M.; Némiga, X. y Lara V. A. 2016. Distribución espacial de trips en aguacate en Coatepec Harinas, Estado de México. Revista Mexicana de Ciencias Agrícolas. 7(4):845-856. <https://doi.org/10.29312/remexca.v7i4.259>.
- 16 Paz, R. y Arrieche, N. 2017. Distribución espacial de *Thrips tabaci* (Lindeman) 1888 (thysanoptera: thripidae) en Quibor, Estado Lara, Venezuela. Bioagro. 29(2):123-128. <https://ve.scielo.org/pdf/ba/v29n2/art06.pdf>.
- 17 Pérez-Constantino, A.; Ramírez-Dávila, J. F.; Gutiérrez-Rodríguez, F. y Pérez-López, D. D. J. 2023. Comportamiento espacial de roya del cafeto en Amatepec, Estado de México. Acta Universitaria 33. <https://doi.org/10.15174/au.2023.3870>.
- 18 Pino-Miranda, E.; Ramírez-Dávila, J. F.; Serrato-Cuevas, R.; Mejía-Carranza, J. y Tapia-Rodríguez, A. 2022. Distribución espacial y temporal del ojo de gallo (*Mycena citricolor*) en cafetales del Estado de México. Revista Mexicana de Fitopatología. 40(3):433-446. Doi: <https://doi.org/10.18781/r.mex.fit.2204-2>.
- 19 Ramírez-Dávila, J. F.; Gonzales-Andujar, J. L. y Porcayo-Camargo, E. 2008. Distribución espacial de las larvas del mosquito verde en un viñedo de regadío en Andalucía, España, utilizando el método de SADIE. Boletín de Sanidad Vegetal. 34(4):607-614. <https://www.researchgate.net/publication/41126167>.
- 20 Ramírez-Dávila, J. F.; Sánchez-Pale, J. R. y León, C. D. 2011. Estabilidad espacio temporal de la distribución del carbón de la espiga del maíz (*Sporisorium reilianum*) en el Estado de México, México. Revista Mexicana de Fitopatología. 29(1):1-14. https://www.scielo.org.mx/scielo.php?pid=S018533092011000100001&script=sci_abstract&tlang=pt.
- 21 Ramírez-Dávila, J. F.; Sánchez-Pale, J. R. y León, C. D. 2011. Estabilidad espacio temporal de la distribución del carbón de la espiga del maíz (*Sporisorium reilianum*) en el Estado de México, México. Revista Mexicana de Fitopatología. 29(1):1-14. <https://scielo.org.mx/pdf/rmfi/v29n1/v29n1a1.pdf>.
- 22 Rengifo, H. G.; Leguizamon, J. E. y Riaño, N. M. 2002. Algunos aspectos biológicos de *Cercospora coffeicola* Chinchiná (Colombia). Rev. Cenicafé. 53(3):169-177. <https://www.cenicafe.org/es/publications/arc053%2803%29169-177.pdf>.
- 23 Sciarretta, A.; Zinni, A.; Mazzocchetti, A. y Trematerra, P. 2008. Análisis espacial de la población de machos de *Lobesia botrana* (Lepidoptera: Tortricidae) en un paisaje

- agrícola mediterráneo en el centro de Italia. Entomología ambiental 37(2):382-390. Doi:10.1603/0046-225x(2008)37[382:saolbl]2.0.co;2.
- 24 Sepúlveda, L. 2016. Caracterización fenotípica de *Mycosphaerella fijiensis* y su relación con la sensibilidad a fungicidas en Colombia. Revista Mexicana de Fitopatología 34(1):1-21. Doi:<https://doi.org/10.18781/r.mex.fit.1507.8>.
- 25 SIAP. 2023. Servicio de Información Agroalimentaria y Pesquera. Anuario estadístico de la producción agrícola. <https://www.gob.mx/siap/acciones-y-programas/produccion-agricola-33119>.
- 26 Tapia-Rodríguez, A.; Ramírez-Dávila, J. F.; Figueroa-Figueroa, D. K, Salgado-Siclan, M. L. y Serrato R. 2020. Análisis espacial de antracnosis en el cultivo de aguacate en el Estado de México. Revista Mexicana de Fitopatología 38(1):132-145. Doi: <https://doi.org/10.18781/r.mex.fit.1911-1>.
- 27 Turechek, W. W. and Madden, L. V. 1999. Spatial pattern analysis and sequential sampling for the incidence of leaf spot on strawberry in Ohio. Plant Disease 83(11):992-1000. Doi:10.1094/PDIS.1999.83.11.992.





Spatial variability of *Mycosphaerella coffeicola* (Cooke) populations in coffee plantations, State of Mexico

Journal Information
Journal ID (publisher-id): remexca
Title: Revista mexicana de ciencias agrícolas
Abbreviated Title: Rev. Mex. Cienc. Agríc.
ISSN (print): 2007-0934
Publisher: Instituto Nacional de Investigaciones Forestales, Agrícolas y Pecuarias

Article/Issue Information
Date received: 01 April 2025
Date accepted: 01 July 2025
Publication date: 18 September 2025
Publication date: Aug-Sep 2025
Volume: 16
Issue: 6
Electronic Location Identifier: e3798
DOI: 10.29312/remexca.v16i6.3798

Categories

Subject: Articles

Keywords:

Keywords:

Mycosphaerella coffeicola
aggregation
geostatistics
ordinary kriging
semivariograms

Counts

Figures: 2

Tables: 2

Equations: 0

References: 27

Pages: 0